Pathogenicity of three genetically distinct and highly pathogenic Egyptian H5N8 avian influenza viruses in chickens

Nahed Yehia,[*] Ahmed M. Erfan,[*] Amany Adel,[*] Ahmed El-Tayeb,[*] Wafaa M. M. Hassan,[*] Ahmed Samy,[*,†] Mohamed E. Abd El-Hack,[‡] Mohamed T. El-Saadony,[§] Khaled A. El-Tarabily,[#,‖‖,1] and Kawkab A. Ahmed[¶]

[*]*Reference Laboratory for Veterinary Quality Control on Poultry Production, Animal Health Research Institute, Agricultural Research Center, Dokki, Giza, 12618, Egypt;* [†]*Immunogenetics, The Pirbright Institute, Surrey, GU24 0NF, UK;* [‡]*Department of Poultry, Faculty of Agriculture, Zagazig University, Zagazig, 44511, Egypt;* [§]*Department of Agricultural Microbiology, Faculty of Agriculture, Zagazig University, Zagazig, 44511, Egypt;* [#]*Department of Biology, College of Science, United Arab Emirates University, Al-Ain, 15551, United Arab Emirates;* [‖‖]*Harry Butler Institute, Murdoch University, Murdoch, 6150, Western Australia, Australia; and* [¶]*Department of Pathology, Faculty of Veterinary Medicine, Cairo University, Giza, 12211, Egypt*

ABSTRACT In late 2016, Egypt encountered multiple cases of the highly pathogenic avian influenza (**HPAI**) virus of the H5N8 subtype. In a previous study, three distinct genotypes, including A/common-coot/Egypt/CA285/2016 (H5N8) (CA285), A/duck/Egypt/SS19/2017 (H5N8) (SS19), and A/duck/Egypt/F446/2017 (H5N8) (F446), were isolated from wild birds, a backyard, and a commercial farm, respectively, during the first wave of infection. In this current study, we investigated the differences in the pathogenicity, replication and transmissibility of the three genotypes and A/chicken/Egypt/15S75/2015 (H5N1) (S75) was used as the control. The intravenous pathogenicity index was between 2.68 and 2.9. The chicken lethal dose 50 values of F446, SS19 and CA285 were $10^{3.7}$, $10^{3.7}$, an 10^4 with a natural route of infection, respectively. These strains took longer than S75 to cause death when infection was carried out through the natural route (HPAI H5N1). After inoculation with the original concentration of 10^5 and 10^6 egg infective dose 50 (**EID_{50}**), F446 had a higher mortality rate with short mean death times of 4, and 7 days, respectively compared with the other H5N8 viruses. Chickens inoculated with F446 and contacted exposed chickens infected with F446 showed the highest viral titer with remarkable differences in all H5N8 tested swabs at 2-4 days postinfection (**dpi**) compared to S75 at 2 dpi. This indicates that F446 had a more efficient transmission and spread from contact exposed birds to other birds. All H5N8 viruses were able to replicate systematically in all organs (trachea, brain, lung, and spleen) of the chicken with high viral titer with significantly different and more pathological changes observed in F446 than in other H5N8 viruses at 2 and 4 dpi. Compared with H5N1, we recorded a significantly high viral titer in the samples obtained from the lung, brain and both cloacal and tracheal swabs at 2 and 4 dpi, respectively and in the samples obtained from the spleen at 2 and 4 dpi among the experimental chicken. The comparative pathogenesis study revealed that in comparison with the other HPAI H5N8 viruses, the genotype F446 was more pathogenic, and showed more efficient viral replication and transmissibility in chickens in Egypt. The genotype F446 also showed a high viral titer than HPAI H5N1 and short mean death time at the third day after inoculation with 10^6 and 10^5 EID50, which revealed a conservation of certain H5N8 genotypes and a decrease in the incidence of H5N1.

Key words: avian influenza, chicken, H5N8, pathogenicity, transmissibility

2022 Poultry Science 101:101662
https://doi.org/10.1016/j.psj.2021.101662

INTRODUCTION

Highly pathogenic avian influenza (**HPAI**) is caused by the H5 subtype of type A influenza virus, a member of the family orthomyxoviridae, of the goose/Guangdong/1996 lineage. The H5 HPAI virus has since been identified for decades before those causing huge economic losses. The zoonotic potential of this virus is also noteworthy. Globally, from January 2003 to December

Received June 23, 2021.
Accepted November 25, 2021.

[1]Corresponding author: ktarabily@uaeu.ac.ae

2020, 862 human infections have been reported for H5N1 with 455 fatalities, and till date, 25 (H5N6) infections have been reported in China with eight fatalities (WHO, 2020). The goose/Guangdong (Gs/GD) lineage viruses, unlike previous HPAI viruses, were isolated from wild birds (Röhm et al., 1995), which may explain their rapid and global spread (Swayne et al., 2016). The Gs/GD lineage has evolved into 10 viral clades (0−9) with multiple subclades (WHO, 2008).

The group of viruses harboring the hemagglutinin gene (**HA**) of clade 2.3.4 acquired different neuraminidase genes (**NA**), including N2, N5, and N8, via reassortment with other local avian influenza viruses. These viruses have been isolated from domestic birds in China, particularly live poultry markets. Clade 2.3.4 has further evolved into 2.3.4.4, which includes the H5N2, H5N6, and H5N8 subtypes that have caused panzootic waves with severe losses to poultry production worldwide (Gu et al., 2011; Zhao et al., 2012; Wu et al., 2014). The HPAI H5N8 clade 2.3.4.4 viruses were first detected in wild migratory waterfowl in China in 2013 (Gu et al., 2011).

Genetic analysis revealed that two distinct genetic groups (A and B) were introduced in Korea in early 2014, likely via migratory birds (Jeong et al., 2014; Lee et al., 2017a). Group A was represented by A/broiler duck/Korea/Buan2/2014, whereas group B was represented by A/breeder duck/Korea/ Gochang1/2014 (Lee et al., 2017a). In late 2014, group A spread to North America via long-distance migratory birds where it reassorted with local low pathogenic avian influenza (**LPAI**) viruses, generating H5N2, among other viruses, which became the predominantly circulating virus in North America in 2014−2015, causing several outbreaks in poultry farms (Pasick et al., 2015; Lee et al., 2016).

Simultaneously, group A also spread westward to Europe and caused widespread outbreaks by the end of 2014 (Bouwstra et al., 2015; Hanna et al., 2015; Harder et al., 2015). By mid-2016, a reassortant HPAI H5N8 clade 2.3.4.4 group B, containing polymerase basic 1 (**PB1**) and 2 (**PB2**), polymerase acidic (**PA**), nucleoprotein (**NP**), and matrix (**M**) segments from Eurasian LPAI, was identified from the Qinghai Lake in China and the Uvs Nuur Lake in South Russia in dead wild birds (Lee et al., 2017b; Li et al., 2017).

These novel viruses further reassorted with Eurasian LPAI viruses and disseminated over a huge geographical area in 2016, including Europe, Africa, Asia, and the Middle East, along migratory waterfowl routes (Lee et al., 2017b). In Egypt, HPAI H5N8 clade 2.3.4.4 group B was first reported in late 2016 in wild birds on the north coast (Kandeil et al., 2017; Selim et al., 2017).

From late 2016 till date, H5N8 has spread all over Egypt and became the predominant HPAI H5 virus in circulation, replacing the H5N1 viruses (Yehia et al., 2020). Genetic analysis has revealed multiple cases of reassortant H5N8 viruses (Salaheldin et al., 2018; Yehia et al., 2018). Three distinct reassorted H5N8 viruses were reported in late 2016 and early 2017 with a different origin of PB2, PB1, PA, and/or NP segments (Yehia et al., 2018). These were A/common-coot/Egypt/CA285/2016 (CA285), which was isolated from wild birds; A/duck/Egypt/SS19/2017 (SS19), which was isolated from backyard ducks; and A/duck/Egypt/F446/2017 (F446), which was isolated from commercial duck farms (Yehia et al., 2018). F446 became the most predominant H5N8 genotype circulating in Egypt, having PA and NP segments similar to those observed in A/mallard/Republic of Georgia/13/2011 (H6N2).

In contrast, the remaining segments were more closely related to A/H5N8 viruses in wild birds from the Uvs Nuur Lake in south Russia (2016) (Yehia et al., 2020). The same reassortment pattern was identified in Germany in wild birds in November 2016 (Pohlmann et al., 2017). The predominance of F446-like genotypes does not exclude the possibility of other genotypes emerging and their route of transmission in the future.

Till date, the reassortment of H5N8 viruses has occurred outside Egypt via wild birds. This study was performed to elucidate the difference between pathogenicity, replication, and transmissibility among the three representative H5N8 genotypes in chickens.

MATERIALS AND METHODS

Viruses

All H5N8 strains used in the present study were isolated during the first wave of H5N8 infection in Egypt, where CA258 was recovered from wild birds in November 2016 (Selim et al., 2017). In contrast, SS19 was obtained from backyard ducks in January 2017 and F446 was recovered from a commercial duck farm in April 2017 (Yehia et al., 2018). All the three genotypes belonged to clade 2.3.4.4.b.

Full genetic characterization revealed that the strains under study have high nucleotide similarity among HA, NA, M, and NS gene segments with a different origin of PB2, PB1, PA, and/or NP segments (Yehia et al., 2018). Furthermore, S75 representing HPAI H5N1 clade 2.2.1.2 isolated from commercial chicken farms in Egypt was used as the control.

In this study, all viruses were propagated by inoculating diluted stock virus solution into the allantoic cavity of 11-day-old specific-pathogen-free embryonated chicken eggs (**SPF-ECEs**) and incubated at 37°C with daily candling. All embryos that died during the first 24 h were excluded; the eggs were then placed at 4°C for at least 4 h. The allantoic fluid was collected, and hemagglutination activity was examined as recommended by the Office International des Epizooties (OIE, 2018). The viruses were titrated in SPF-ECEs using egg infective dose 50 (EID_{50}) per mL, which was calculated using the Reed and Muench method (Reed and Muench, 1938).

Animal Experiments

All animal experiments were conducted in negative-pressure BSL3 isolators at the Reference Laboratory for Veterinary Control on Poultry Production (**RLQP**) of

the Animal Health Research Institute (**AHRI**), Agricultural Research Center, Giza, Egypt. All experiments were approved by the Scientific and Biosafety Committee of RLQP, AHRI, Egypt. Additionally, experiments were conducted as per the recommendations and guidelines of the Ministry of Agriculture and Land Reclamation, Egypt.

Three experiments were conducted to examine the pathogenicity, replication, and transmissibility patterns of the three H5N8 viruses and one H5N1 virus.

Experiment 1

The intravenous pathogenicity index (**IVPI**) was conducted to assess the pathogenicity of each virus. It was measured following the procedure of the OIE (2018). Briefly, ten 6-wk-old SPF chickens (white leghorn) were inoculated with 0.1 mL of each virus at 6 $\log_2$ hemagglutination (**HA**) titer. Clinical signs, including respiratory manifestations, depression, diarrhea, cyanosis of the exposed skin or wattles, facial edema, and/or nervous signs, were scored daily for 10 d.

Birds without the signs above were considered normal (scored 0), whereas those with one sign were considered sick (scored 1), and those with more than one sign were considered severely sick (scored 2); and birds that died were scored 3.

Experiment 2

This experiment aimed to detect the pathogenesis of each virus using a natural route of inoculation by measurement of chicken lethal dose 50 (CLD_{50}), mortality rate, mean death time (**MDT**), and survival curve of each virus at different dilutions.

Four dilutions (10^3−10^6 EID_{50}/100 μL) for each virus were prepared. Each dilution was intranasally inoculated in both the nares and choanal cleft as a natural route of infection into five 4-wk-old chickens, which were observed for 10 d. Deaths were recorded twice per day. Birds with severe depression and those about to die were euthanized and counted as deceased birds. The survival curve was analyzed statistically using the Kaplan−Meier method. The CLD50 was calculated according to the method elucidated by Reed and Muench (1938). The mortality rate and MDT were calculated according to the method elucidated by Swayne et al. (1998).

$$\text{MDT} = \frac{\text{number of deaths at (A) day x A day} + \text{number of deaths at (B) day x B day} + \text{etc.}}{\text{Total number of deaths}}$$

Experiment 3

This experiment was conducted to evaluate the replication and propagation of each virus in infected chicken and contact exposed chicken in different organs and investigating the transmissibility of each virus.

It was conducted by inoculating each virus strain (10^6 EID_{50}/100 μL) into 10 SPF chickens, and on the next day, three noninfected chickens of the same age were introduced to each group as contact exposed. Cloacal and tracheal swabs were collected from all birds at 2 and 4 d postinfection (dpi) for virus titration.

For virus titration and histopathological examination, the lung, spleen, and brain were aseptically collected from three infected birds from each group at 2 and 4 dpi or at death.

Quantifying Viral Shedding and Replication Levels in Different Organs

For viral titration, the collected swabs and 0.1 g of the collected organs were subjected to RNA extraction using the QIAamp Viral RNA Mini Kit (Qiagen, GmbH, Hilden, Germany) following the manufacturer's recommendations.

Briefly, the collected tissues were homogenized with an equal volume of phosphate-buffered saline using the tissue lyser LT (Qiagen, GmbH, Hilden, Germany) and it was then subjected to three successive freeze-thaw cycles. Samples were then centrifuged at 12,000 x g for 10 min to separate the supernatant. The swabs collected from each bird were individually placed in a viral transport medium.

Individual swab samples from each chicken were subjected to ribonucleic acid (**RNA**) extraction. RNA purity was measured using a Nano DropTM 2000 spectrophotometer (Thermo Fisher Scientific, Waltham, MA). The quantitect probe reverse transcriptase-polymerase chain reaction (**RT-PCR**) Kit (Qiagen) was employed for reverse transcription (RT) and amplification of the H5 gene using specific primers and a TaqMan probe as previously described by Löndt et al. (2008) (Table 1). Each real-time RT-PCR run included a 10-fold serial dilution of each strain tested to serve as a calibrator along with the no-template controls.

Histopathological Evaluation

Specimens from the trachea, lung, spleen, and brain were collected from birds in all experimental groups at 2 and 4 dpi and fixed in 10% neutral buffered formalin. Next, they were routinely processed, sectioned at 5-μm thickness, and stained with hematoxylin and eosin (Landmann et al., 2021) for subsequent histopathological examination using a light microscope (Olympus BX50, Tokyo, Japan).

Lesions in the trachea, lungs, spleen, and brain of three birds from each group at 2 and 4 dpi were microscopically examined, scored and evaluated on a scale

Table 1. Primers used for viral titration by real-time reverse transcription-polymerase chain reaction (RT-PCR).

Name	Primer sequence
Sep1	5′-AGATGAGTCTTCTAACCGAGGTCG-3′
Sep2	5′-TGCAAAAACATCTTCAAGTCTCTG-3′
Probe SePRO	[FAM]-TCAGGCCCCCTCAAAGCCGA-[TAMRA]

from 0 to 3 based on lesion severity grade (i.e., mild, moderate, or severe) as follows: 0 = no changes, 1 = mild, 2 = moderate, and 3 = severe (Landmann et al., 2021).

Statistical Analysis

Data were coded and entered using statistical package for the social sciences version 26 (IBM Corp., Armonk, NY). Comparisons between groups were performed using analysis of variance with multiple comparisons post hoc test when comparing more than 2 groups (Chan, 2003).

The negative RT-PCR results were treated as missed data because these had no numerical value that could be used for quantitative data analysis. Survival curves were plotted using the Kaplan−Meier method and compared using the log-rank test (Chan, 2004). *P*-values of <0.05 were used to denote statistical significance.

RESULTS

The A/common-coot/Egypt/CA285/2016 (H5N8) (CA285), A/duck/Egypt/SS19/2017 (H5N8) (SS19), and A/duck/Egypt/F446/2017 (H5N8) (F446) viruses isolated from swabs collected from wild birds, a backyard, and a commercial farm, respectively, during the first wave of H5N8 in Egypt were used in this study. The A/chicken/Egypt/15S75/2015 (H5N1) (S75) was used as the control.

Experiment 1

Ten 6-wk-old chickens were intravenously inoculated with 0.1 mL of each virus at 6 $\log_2$ hemagglutination (HA) titer of each of the four viruses. The IVPI was found to be 2.73, 2.92, 2.78, and 2.68 for S75, CA285, SS19, and F446, respectively. The mortality rate was 100% at 2, 2, and 3 dpi with MDTs of 1.5, 2 and 2.5 ds for S75, CA285, and SS19, respectively, and it was 90% at 4 dpi for F446 with an MDT of 3 d.

Experiment 2

To investigate the pathogenesis of the virus we measured the CLD_{50}, mortality rate, MDT, and survival curve using the natural route of infection. As a natural route of infection, five chickens were intranasally inoculated with 10^3−10^6 EID_{50} of each strain and observed for 10 d. The CLD_{50} of S75 was found to be more than 10^3, whilst the CLD_{50} of F446, SS19, and CA285 was $10^{3.7}$, $10^{3.7}$, and 10^4, respectively.

The Kaplan−Meier survival curve with a median survival and unpaired log-rank test were used to calculate and compare survival between the groups (Figure 1). The differences of all survival curves between groups were significant with *P*-value <0.05 (Table 2).

All chickens inoculated with 10^6 EID_{50} of S75 at 4 dpi showed an MDT of 3 d, whilst chickens inoculated with 10^6 EID_{50} of SS19 and F446 died at 5 dpi with an MDT of 4 d. In addition, all chickens inoculated with 10^5 EID_{50} of S75, F446, and SS19 died at 4, 9, and 10 dpi with MDTs of 3, 7, and 8 d, respectively. Meanwhile, 80% of the birds died after inoculation with 10^5 EID50 of CA285 at 9 dpi with an MDT of 7 d.

With one $\log_{10}$ reduction (10^4 EID_{50}), 80% of the birds inoculated with S75 died at 7 dpi with an MDT of 6 d and 60% of the birds inoculated with F446 and SS19 died at 9 dpi with MDTs of 7.5 and 8 d, respectively. Whereas CA258 was fatal in only 40% of the birds at 9 dpi with an MDT of 8 d (Figure 1). In addition, 80% of the chickens died with 10^3 EID_{50} of S75, whereas only 60% of the chickens inoculated with 10^3 EID_{50} of F446

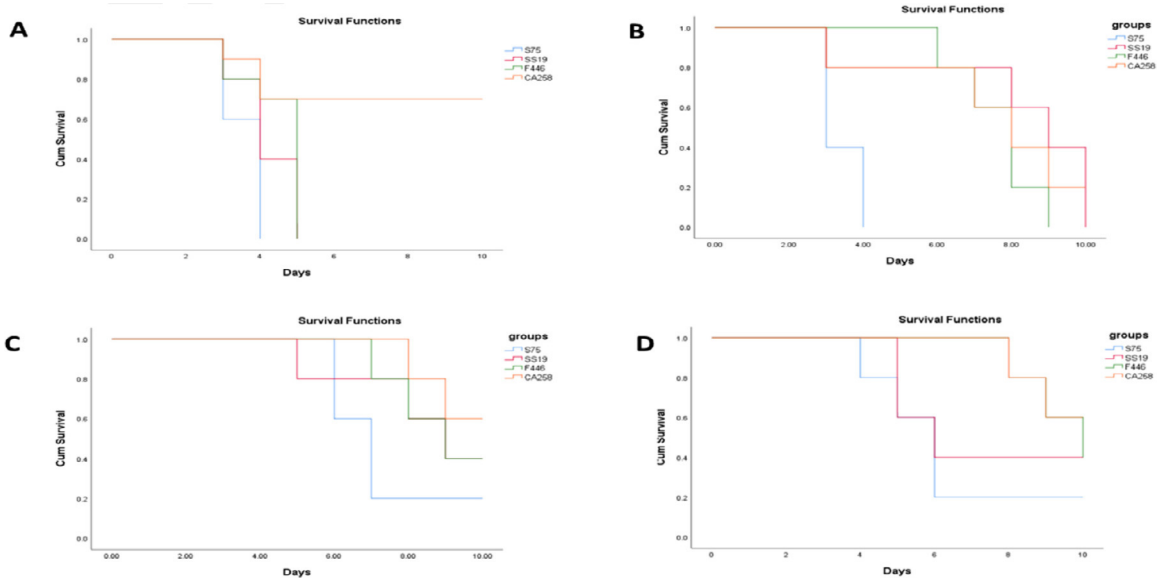

Figure 1. The survival curve of chickens inoculated intranasally as a natural route of infection with 10^6 (A), 10^5(B), 10^4 (C), and 10^3(D) egg infective doses of, HPAI CA285, F446, SS19, and S75 represented by a closed diamond, closed square, closed triangle, and cross, respectively.

Table 2. A Kaplan-Meier survival curve with the calculation of median survival and unpaired log-rank test for significant differences in the survival between the HPAI CA285, F446, SS19, and S75 with 10^6 (A), 10^5(B), 10^4 (C), and 10^3(D) egg infective dose.

A.

	Mean survival	Standard Error	95% confidence interval	
S75	3.600	0.163	3.280	3.929
SS19	4.200	0.249	3.711	4.689
F446	2.500	0.269	3.973	5.027
CA258	8.100	0.921	6.294	9.906
Overall	5.100	0.374	4.367	5.833

Overall comparison

	CHL-square	Df	*P* value
Log Rank (mantel-cox)	6.762	1	0.009

Test of quality of survival distribution for the different levels of groups.

B.

Overall comparison

	CHL-square	Df	*P* value
Log rank (mantel-cox)	19.316	3	<0.001

The vector of trend weights is -3-, -1-, 1, and 3. This is the default.

	Mean*				Median			
	Estimate	Standard error	95% confidence interval		Estimate	Std. error	95% confidence interval	
			Lower bound	Upper bound			Lower bound	Upper bound
S75	3.400	0.163	3.080	3.720	3.000			
SS19	8.000	0.869	6.296	9.704	9.000	0.775	7.482	10.518
F446	7.600	0.340	6.934	8.266	8.000	0.316	7.380	8.620
CA258	7.400	0.764	5.902	8.898	8.000	0.775	6.482	9.518
Overall	6.600	0.422	5.773	7.427	7.000	0.527	5.967	8.033

C.

Overall comparison

	CHL-Square	Df	*P* value
Log Rank (mantel-cox)	8.796	3	0.032

Test of quality of survival distribution for the different levels of groups.

	Mean*				Median			
	Estimate	Standard error	95% confidence interval		Estimate	Standard error	95% confidence interval	
			Lower bound	Upper bound			Lower bound	Upper bound
S75	7.200	0.465	6.289	8.111	7.000	0.316	6.380	7.620
SS19	8.400	0.578	7.250	9.550	9.000	0.775	7.482	10.518
F446	8.800	0.369	8.077	9.523	9.000	0.775	7.482	10.518
CA258	9.400	0.253	8.904	9.896				
Overall	8.450	0.252	7.955	8.945	9.000	0.516	7.988	10.012

D.

Overall comparison

	CHL-square	Df	*P* value
Log Rank (mantel-cox)	8.280	3	0.041

	Mean*				Median			
	Estimate	Standard error	95% confidence interval		Estimate	Standard error	95% confidence interval	
			Lower bound	Upper bound			Lower bound	Upper bound
S75	6.200	0.645	4.936	7.464	6.000	0.316	5.380	6.620
SS19	6.200	0.732	5.765	8.635	6.000	0.775	4.482	7.518
F446	9.400	0.277	8.857	9.943	10.000	0.775	8.482	11.518
CA258	9.400	0.253	8.904	9.896				
Overall	8.050	0.348	7.368	8.732	9.000	0.787	7.458	10.542

*Test of quality of survival distribution for the different levels of groups.

and SS19 and 40% of the chickens inoculated with CA285 died at 6 to 10 dpi (Figure 1).

Experiment 3

To measure the viral shedding in swabs and different organs of each virus, swabs, and lung, spleen, and brain samples were collected at 2 and 4 dpi with 10^6 EID_{50} of each virus. Viral titers in all tested samples infected with F446 were significantly higher than those in samples infected with CA285 and SS19, correlating with significantly more transmission to the contact exposed cohoused birds (Figure 2 and Table 3).

Furthermore, F446-infected birds had significantly higher viral titers in the swabs at 2 dpi and spleen at 2 and 4 dpi than S75-infected birds. Furthermore, F446-infected birds had significantly higher viral titers in the lung and brain samples at 4 dpi than S75-infected birds (Figure 2 and Table 3).

Two of the three contact exposed birds infected with S75 died at 4 and 5 dpi, and one contact exposed bird infected with F446 and SS19 died at 6 dpi. A significantly high viral titer was noted in F446 compared with those in SS19 and CA285 at 2 and 4 dpi, respectively, and S75 at 2 dpi (Figure 3 and Table 3). F446 was more efficiently transmitted to contact exposed co-housed birds than SS19 and CA285 at 2 and 4 dpi, respectively, and compared to S75 at 2 dpi.

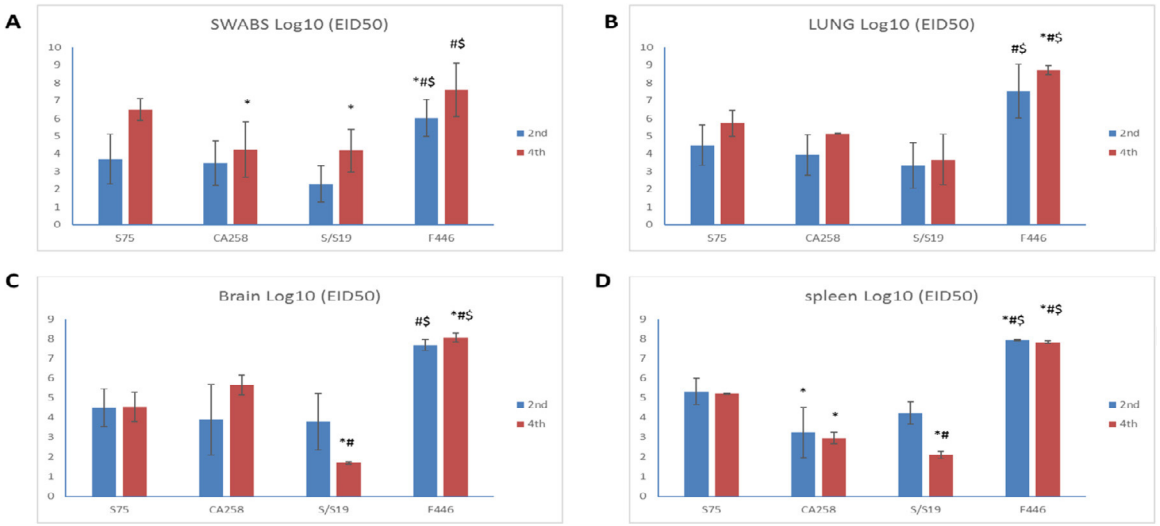

Figure 2. Viral titers in swabs, lung, brain, and spleen tissues of infected chickens at 2 and 4 d postinfection (dpi) with S75, CA285, SS19, and F446. *Statistically significant compared to the corresponding value in S75 ($P < 0.05$), #Statistically significant compared to the corresponding value in CA258 ($P < 0.05$) and $Statistically significant compared to the corresponding value in S/S19 ($P < 0.05$). EID50; egg infective dose 50.

Table 3. *P* value and significant different of the three Egyptian H5N8 avian influenza viruses in swabs and different organs of infected and infected contact exposed chickens.

Samples		S75	CA258	S/S19	F446	*P* value
Swabs Log_{10} (EID50)	2nd	3.7 ± 1.4	3.47 ± 1.26	2.3 ± 1.01	6.02 ± 1.03*,#,$	<0.001
	4th	6.49 ± 0.62	4.25 ± 1.57 *	4.19 ± 1.2 *	7.6 ± 1.52#,$	<0.001
Lung Log_{10} (EID50)	2nd	4.49 ± 1.15	3.94 ± 1.13	3.32 ± 1.28	7.54 ± 1.5#,$	0.016
	4th	5.72 ± 0.74	5.14 ± 0.04	3.67 ± 1.44	8.71 ± 0.25 *,#,$	<0.001
Brain Log_{10} (EID50)	2nd	4.51 ± 0.96	3.89 ± 1.79	3.78 ± 1.44	7.67 ± 0.27 #,$	0.016
	4th	4.53 ± 0.75	5.65 ± 0.49	1.7 ± 0.07 *,#	8.06 ± 0.22 *,#,$	<0.001
Spleen Log_{10} (EID50)	2nd	5.32 ± 0.66	3.23 ± 1.28 *	4.22 ± 0.56	7.92 ± 0.02 *,#,$	<0.001
	4th	5.2 ± 0.03	2.95 ± 0.29 *	2.1 ± 0.17 *,#	7.82 ± 0.07 *,#,$	<0.001
Contact swab Log_{10} (EID50)	2nd	3.61 ± 0.1		2.06 ± 0.08 *	5.81 ± 0.53 *,$	0.003
	4th	3.58 ± 1.66	1.69 ± 0.09	1.68 ± 0.45	5.52 ± 0.08 #,$	0.029

Values are presented as mean ±SD. EID50; egg infective dose 50.
*Statistically significant compared to the corresponding value in S75 ($P < 0.05$).
#Statistically significant compared to the corresponding value in CA258 ($P < 0.05$).
$Statistically significant compared to the corresponding value in S/S19 ($P < 0.05$).*P* values of <0.05 were used to denote statistical significance.

Histopathological Investigations

Light microscopic examination of the tracheal samples obtained from control chickens (2 and 4 dpi) revealed a normal histological architecture of tracheal layers (Figure 4A). However, mild changes were noted in samples obtained from chickens inoculated with CA285 because the examined trachea exhibited mild edema in the lamina propria/submucosa (Figure 4C). Alternatively, trachea of chickens inoculated with S75 showed small focal necrosis of the lamina epithelialis of tracheal mucosa (Figure 4B), with slight edema in the lamina propria.

Furthermore, mild congestion of the mucosal blood capillaries (Figure 4D) was the only finding in the trachea of chickens inoculated with SS19 (2 dpi). Meanwhile, the prominent histopathological changes observed

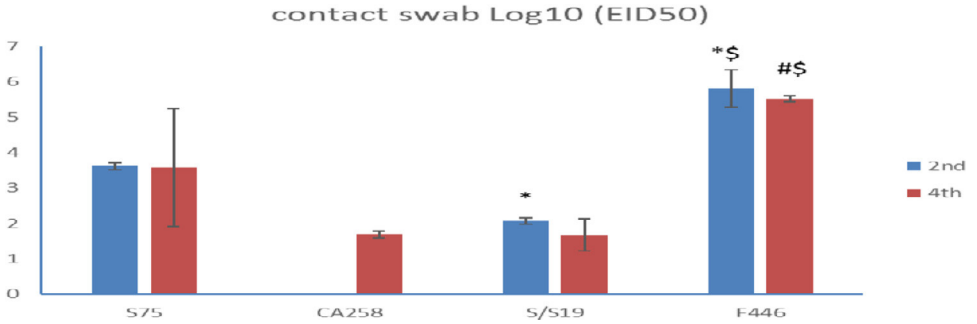

Figure 3. Viral titers in swabs of infected contact exposed chickens at 2 and 4 d postinfection (dpi) with S75, CA285, SS19, and F446. *Statistically significant compared to the corresponding value in S75 ($P < 0.05$), #Statistically significant compared to the corresponding value in CA258 ($P < 0.05$) and $Statistically significant compared to the corresponding value in S/S19 ($P < 0.05$). EID50; egg infective dose 50.

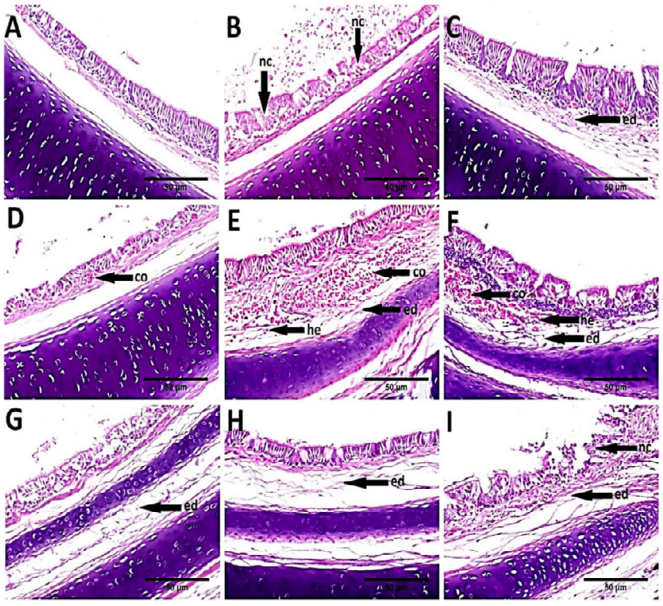

Figure 4. Photomicrographs of histological H&E-stained tracheal sections of chickens; 2 d postinfection (dpi) (A–E), and 4 dpi (F–I): (A) control showing the normal histological architecture of tracheal layers. (B) S75 (H5N1), showing small focal necrosis of lamina epithelial of tracheal mucosa (nc). (C) CA285 group showing mild edema in lamina propria/submucosa (ed). (D) S/S19, showing mild congestion of mucosal blood capillaries (co). (E) F446, showing congestion of mucosal blood vessel (co), edema in lamina propria/submucosa (ed) associated with focal hemorrhage (he). (F) S75, showing congestion of mucosal blood vessel (co), edema in lamina propria/submucosa (ed) and hemorrhage (he). (G) CA285, showing submucosal edema in (ed). (H) S/S19, showing edema in lamina propria/submucosa (ed). (I) F446, showing focal mucosal necrosis (nc) and desquamation as well as edema in lamina propria (ed) (scale bar, 50 μm).

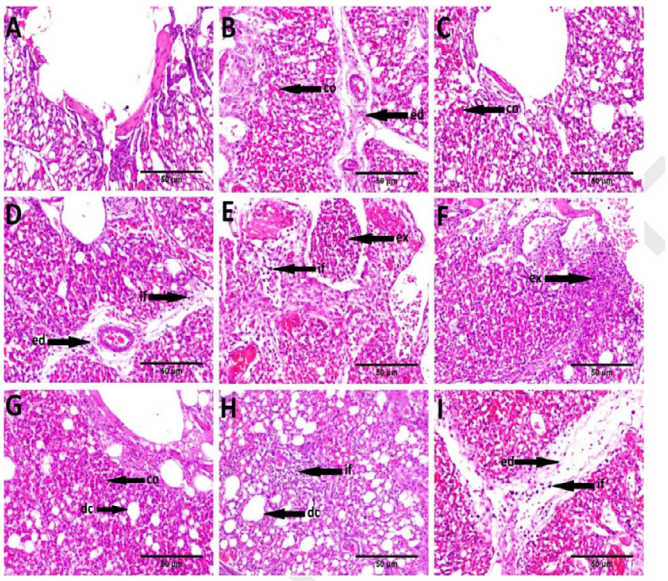

Figure 5. Photomicrographs of histological H&E-stained lung sections of chickens; 2 d postinfection (dpi) (A–E), and 4 dpi (F–I): (A) control showing the normal histology of parabronchus and air capillaries. (B) S75 (H5N1), showing congestion of blood capillaries (co) with interlobular and perivascular edema (ed). (C) CA285, showing mild congestion of blood capillaries (co). (D) S/S19, showing interlobular edema (ed) associated with inflammatory cells infiltration (if). (E) F446, showing impaction of the parabronchus lumen with inflammatory exudate (ex). Note inflammatory cells infiltration (if). (F) S75, showing focal necrosis of air capillaries associated with inflammatory exudate (ex). (G) CA285, showing congestion of blood capillaries (co) and dilatation of some air capillaries (dc). (H) S/S19, showing focal mononuclear inflammatory cells infiltration (if) and dilatation of some air capillaries (dc). (I) F446, showing interstitial pneumonia exhibited by severe interlobular edema (ed) associated with inflammatory cells infiltration (if) (scale bar, 50 μm).

in the trachea of birds inoculated with F446 were congestion of the mucosal blood vessels and edema in the lamina propria/submucosa associated with focal submucosal hemorrhage (Figure 4E).

In addition, at 4 dpi, the examined tracheal sections obtained from birds inoculated with S75 revealed congestion of the mucosal blood vessels, edema in the lamina propria/submucosa, and hemorrhage in the lamina propria (Figure 4F). Mild histopathological damage was observed in the trachea of chickens inoculated with either CA285 or SS19 and the examined sections showed mild edema in the lamina propria/submucosa (Figure 4G and H). However, severe lesions characterized by congestion of the mucosal blood vessels, focal mucosal necrosis and desquamation, as well as edema in the lamina propria (Figure 4I) were observed in the trachea of chickens inoculated with F446.

Regarding the lungs, the examined sections obtained from control chickens revealed a normal histological structure of the parabronchus and air capillaries (Figure 5A). At 2 dpi, histopathological examination of lung tissue of chickens inoculated with S75 (H5N1) showed congestion of the blood capillaries and vessels associated with interlobular and perivascular edema (Figure 5B). Meanwhile, mild congestion of the blood capillaries was the only histopathological finding observed in the lungs of CA285-inoculated chickens (Figure 5C). However, lung sections from chickens infected with SS19 showed congestion of the blood capillaries and interlobular edema associated with inflammatory cell infiltration (Figure 5D). Alternatively, severe histopathological lesions were observed in the lungs of chickens inoculated with F446. The lesions exhibited impaction of the parabronchus lumen with necrotic and inflammatory exudates associated with the infiltration of inflammatory cells (mainly mononuclear cells and heterophils) (Figure 5E). Furthermore, at 4 dpi, the lungs of birds inoculated with S75 showed focal necrosis of air capillaries associated with inflammatory exudates (Figure 5F). Meanwhile, sections obtained from CA285-inoculated chickens exhibited congestion of the blood capillaries and dilatation of some air capillaries (Figure 5G).

The lungs of chickens inoculated with SS19 revealed focal mononuclear inflammatory cell infiltration and dilatation of some air capillaries (Figure 5H). Severe alterations were observed in the lungs of chickens inoculated with F446; these alterations, were summarized as interstitial pneumonia, marked interlobular edema, inflammatory cell infiltration (Figure 5I), congestion of the blood capillaries, and focal pulmonary hemorrhage.

Microscopically, the spleen of control chickens (2 and 4 dpi) showed a normal histological structure of

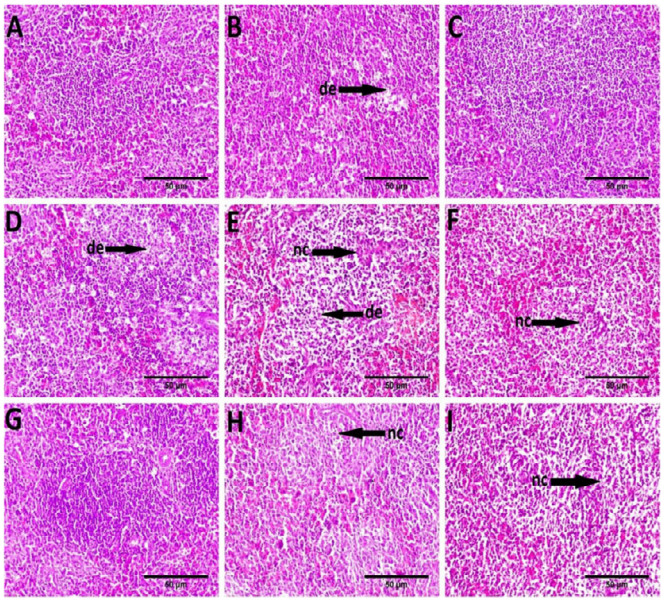

Figure 6. Photomicrographs of histological H&E stained spleen sections of chickens; 2 d postinfection (dpi) (A–E), and 4 dpi (F–I): (A) control showing the normal histology of lymphoid follicles. (B) S75 (H5N1), showing lymphocytic necrosis and depletion (de). (C) CA285, showing normal lymphoid follicles. (D) S/S19, showing mild lymphocytic necrosis and depletion (de). (E) F446, showing fibrinoid necrosis (nc) associated with lymphocytic depletion (de). (F) S75, showing lymphocytic necrosis (nc). (G) CA285, showing no histopathological alterations. (H) S/S19, showing moderate lymphocytic necrosis (nc). (I) F446, showing fibrinoid necrosis (nc) (scale bar, 50 μm).

lymphoid follicles (Figure 6A). At 2 dpi, the spleen of chickens infected with S75 showed lymphocytic necrosis and depletion of some lymphoid follicles (Figure 6B). Meanwhile, the examined sections obtained from CA285-inoculated birds showed normal lymphoid follicles (Figure 6C). Mild lymphocytic necrosis and depletion were observed in the spleen of SS19-infected chickens (Figure 6D). The spleen of chickens infected with F446 showed fibrinoid necrosis associated with lymphocytic necrosis and depletion (Figure 6E). In addition, at 4 dpi, the examined spleen of chickens inoculated with S75 showed lymphocytic necrosis (Figure 6F) of some lymphoid follicles. Meanwhile, no histopathological alterations were observed in sections obtained from CA285-inoculated chickens (Figure 6G). Moderate lymphocytic necrosis was observed in the spleen of chickens inoculated with SS19 (Figure 6H). Adversely, the spleen of chickens infected with F446 showed more severe changes characterized by fibrinoid necrosis, lymphocytic necrosis and depletion (Figure 6I).

Microscopic examination of the brain sections of control chickens (2 and 4 dpi) revealed normal histology of the brain parenchyma (Figure 7A). Meanwhile, at 2 dpi, the examined brain tissue of chickens inoculated with S75 (H5N1) showed cellular edema and vacuolation of neurons (Figure 7B), necrosis of some neurons, and neuronophagia. Brain sections obtained from chickens inoculated with CA285 revealed normal tissue without histopathological changes (Figure 7C). In contrast, the remaining experimental groups (SS19 and F446 [2 dpi] and S75, CA285, SS19, and F446 [4 dpi]) showed comparable histopathological alterations characterized by necrosis of some neurons (Figure. 7D–I) and neuronophagia. The histopathological alterations are summarized and graded according to their severity (Table 4).

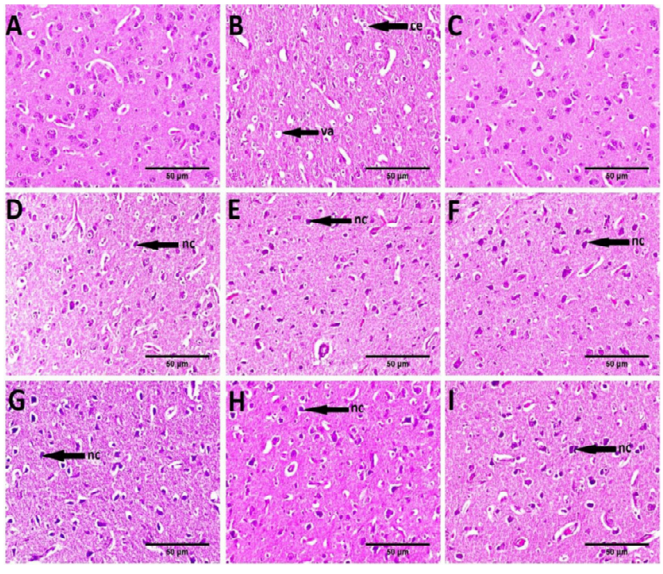

Figure 7. Photomicrographs of histological H&E stained brain sections of chickens; 2 d postinfection (dpi) (A–E), and 4 dpi (F–I): (A) control showing the normal histology of brain parenchyma. (B) S75 (H5N1), showing cellular edema (ce) and vacuolation of neurons (va). (C) CA285, showing no histopathological changes. (D) S/S19; (E) F446; (F) S75; (G) CA285; (H) S/S19; (I) F446, showing necrosis of some neurons (nc) (scale bar, 50 μm).

DISCUSSION

Since May/June 2016, the HPAI H5N8 clade 2.3.4.4b has been causing panzootic waves across Asia, Europe, the Middle East, and Africa (Kleyheeg et al., 2017; OIE, 2017). In Egypt, the virus was first detected in wild birds in the northern region in late 2016 (Selim et al., 2017); it has since then spread all over Egypt and has been isolated from several different poultry production sectors causing massive economic losses (Yehia et al., 2020).

A few months after emergence of the virus in Egypt, a genotyping study revealed a multiple incursion pattern of HPAI H5N8 viruses in Egypt (Salaheldin et al., 2018; Yehia et al., 2018). The first few genotypes were recovered from wild birds in November 2016 (CA285) (Selim et al., 2017), followed by those recovered from backyard ducks in January 2017 (SS19) and commercial duck farms in April 2017 (F446) (Yehia et al., 2018).

These genotypes showed high nucleotide similarity at the level of HA, NA, M, and NS gene segments close to the 2.3.4.4 group B Russia–Mongolia 2016 reassortant isolates e.g., (A/great crested grebe/Uvs-Nuur Lake/341/2016 [H5N8]), with PB2, PB1, PA, and/or NP segments originating from different influenza viruses circulating in Asia and Europe (Yehia et al., 2018). In the present study, we investigated the differences in the

Table 4. Histopathologic lesion scoring in the different organs of birds in different experimental groups.

Histopathological lesions	Control		S75		CA285		S/S19		F446	
	2dpi	4dpi	2dpi	4dpi	2dpi	4dpi	2dpi	4dpi	2dpi	4dpi
Trachea										
Congestion	0.0 ± 0.0	0.0 ± 0.0	1.7 ± 0.6	2.0 ± 0.0	0.0 ± 0.0	1.3 ± .6	1.3 ± 0.6	1.7 ± 0.6	1.7 ± 0.6	1.3 ± 0.6
Edema in lamina propria/submucosa	0.0 ± 0.0	0.0 ± 0.0	0.7 ± 0.6	1.7 ± 0.6	0.7 ± 0.6	1.0 ± 0.0	0.7 ± 0.6	1.7 ± 0.6	1.7 ± 0.6	2.0 ± 0.0
Hemorrhage	0.0 ± 0.0	0.0 ± 0.0	0.0 ± 0.0	2.0 ± 0.0	0.0 ± 0.0	0.0 ± 0.0	0.0 ± 0.0	0.0 ± 0.0	1.7 ± 0.6	1.0 ± 0.0
Focal mucosal necrosis	0.0 ± 0.0	0.0 ± 0.0	1.0 ± 0.0	1.0 ± 0.0	0.0 ± 0.0	0.0 ± 0.0	0.0 ± 0.0	0.0 ± 0.0	0.0 ± 0.0	2.0 ± 0.0
Lungs										
Congestion	0.0 ± 0.0	0.0 ± 0.0	2.3 ± 0.6	3.0 ± 0.0	1.7 ± 0.6	2.0 ± 0.0	1.7 ± 0.6	2.0 ± 0.0	2.0 ± 0.0	3.0 ± 0.0
Interstitial edema	0.0 ± 0.0	0.0 ± 0.0	2.0 ± 0.0	2.0 ± 0.0	0.0 ± 0.0	1.0 ± 0.0	1.7 ± 0.6	2.0 ± 0.0	2.0 ± 0.0	3.0 ± 0.0
Inflammatory cells infiltration	0.0 ± 0.0	0.0 ± 0.0	2.0 ± 0.0	2.7 ± 0.6	0.0 ± 0.0	0.7 ± 0.6	0.7 ± 0.6	1.0 ± 0.0	2.7 ± 0.6	2.7 ± 0.6
Necrosis and exudate in parabronchus	0.0 ± 0.0	0.0 ± 0.0	0.0 ± 0.0	2.0 ± 0.0	0.0 ± 0.0	0.0 ± 0.0	0.0 ± 0.0	0.7 ± 0.6	1.7 ± 0.6	2.0 ± 0.0
Spleen										
Lymphocytic necrosis and depletion	0.0 ± 0.0	0.0 ± 0.0	1.0 ± 0.0	2.0 ± 0.0	0.0 ± 0.0	0.7 ± 0.6	1.0 ± 0.0	1.7 ± 0.6	2.0 ± 0.0	2.7 ± 0.6
Fibrinoid necrosis	0.0 ± 0.0	0.0 ± 0.0	0.0 ± 0.0	0.7 ± 0.6	0.0 ± 0.0	0.0 ± 0.0	0.0 ± 0.0	0.7 ± 0.6	1.7 ± 0.6	2.0 ± 0.0
Brain										
Necrosis of neurons	0.0 ± 0.0	0.0 ± 0.0	1.0 ± 0.0	2.0 ± 0.0	0.0 ± 0.0	1.0 ± 0.0	1.7 ± 0.6	1.7 ± 0.6	2.0 ± 0.0	2.7 ± 0.6
Neuronophagia	0.0 ± 0.0	0.0 ± 0.0	1.0 ± 0.0	2.0 ± 0.0	0.0 ± 0.0	0.7 ± 0.6	0.7 ± 0.6	1.7 ± 0.6	1.7 ± 0.6	2.0 ± 0.0
Cellular edema and vacuolation	0.0 ± 0.0	0.0 ± 0.0	2.0 ± 0.0	1.0 ± 0.0	0.0 ± 0.0	0.0 ± 0.0	0.0 ± 0.0	0.0 ± 0.0	0.7 ± 0.6	0.0 ± 0.0

Data are shown as mean ± SD; one-way analysis of variance (ANOVA) was used to determine differences between groups. (Number of birds/group/d = 3).

Histopathological lesion score was evaluated on a scale from 0 to 3 based on lesion severity grade (i.e., mild, moderate, or severe) as follows: 0 = no changes, 1 = mild, 2 = moderate, and 3 = severe. dpi; days postinfection.

pathogenicity, replication, and transmissibility of the three aforementioned viruses in chickens. Therefore, in chickens infected with viruses representing these different genotypes, the IVPI, CLD50, percentage mortality, MDT, viral shedding, dissemination in different organs, transmissibility, and micropathogenicity were investigated.

The results showed that all tested strains were HPAI with IVPIs ranging from 2.68 to 2.9, which corresponds to HA gene sequencing, confirming the presence of multiple basic amino acid motifs PLREKRRKR/GLF at the cleavage site (Yehia et al., 2018). The CLD50 of F446 and SS19 was found to be $10^{3.7}$ and that of CA285 was found to be 10^4 by a natural route of infection. However, F446 caused 90% mortality at 4 dpi with an MDT of 3 d compared with CA285 and SS19, which caused 100% mortality at 2 and 3 dpi with MDTs of 2 and 2.5 d, respectively. This finding was closer to that observed for S75 (HPAI H5N1) that also caused 100% mortality at 2 dpi with an MDT of 1.5 d. However, mortality was delayed with respect to intranasal inoculation as a natural route of infection compared with S75 strains, with comparable results for CA285, F446 and SS19 with a high infection dose. In addition, remarkably lower mortality was observed in H5N8-inoculated naive contact exposed birds. Intravenous injection of influenza viruses into chickens allows direct exposure of different organs beyond the natural route of infection (Swayne et al., 1994), which can explain the comparable results of IVPI findings.

Meanwhile, intranasal inoculation represents the natural route of infection with delayed onset of mortality and lower transmissibility than HPAI H5N1. The same difference was observed between HPAI H5N1 and the Korean and Japanese H5N8 viruses (Song et al., 2015; Tanikawa et al., 2016).

Furthermore, compared with other H5N8 viruses, intranasal inoculation as a natural route of infection for 10^6 and 10^5 of F446 showed 100% mortality at 5 and 9 dpi with shorter MDTs of 4 and 7 d, respectively, than other H5N8 viruses, indicating the highly pathogenic effect of F446. Swabs collected from chickens inoculated with F446 at 2 and 4 dpi showed higher viral titers with a significant difference than those observed for swabs from chickens inoculated with other H5N8 viruses. In the present study also, higher viral titer with significant differences in swabs collected from contact exposed chickens infected with F446 at 2 and 4 dpi than in those infected with SS19 and CA285 at 2 and 4 dpi , respectively, were detected. These results indicated the higher transmissibility of F446 to contact exposed birds and higher spread from such contact exposed birds to other birds.

The increased transmissibility of F446 compared with that of other H5N8 viruses may be because of the more adapted reassorted polymerase complex virus that induces lower interferon expression, which allows a more prolonged infection and viral shedding, leading to increased viral transmission than the un-adapted influenza polymerase complex. This results in the generation of defective interfering influenza viral RNA and nonfunctional viral RNA, which induces the activation of interferon and enhances the innate immune response (Vigeveno et al., 2020).

Furthermore, there are numerous avian influenza subtypes, including H5N1, H5N8, and H9N2 in Egypt (Hassan et al., 2020). Several future reassortments have been predicted, as recorded in the novel reassortant H5N2 that showed 98 to 99% similarity with F446, suggesting that F446 is the donor virus and N2 from Egyptian H9N2 (Hagag et al., 2019). Furthermore, F446 exhibited 100% mortality of 10^6 and 10^5 in higher MDTs of 4 and 7 d, respectively, compared with S75 of 10^6 and 10^5 that caused 100% mortality at an MDT of 3 d, increasing the transmissibility of F446 compared with that of S75. Higher viral titers with significant

differences than those observed for S75 in the swabs at 2 dpi were noted. This may explain the increased incidence of H5N8 compared with that of H5N1 in 2017−2019 (Kandeil et al., 2019; Hassan et al., 2020).

Silvano et al. (1997) reported that different H5N8 strains cause systemic replication with histopathological changes in different organs, resulting in necrotizing lesions. Moreover, the pathogenesis of infection involves invasion of the virus through the blood-brain barrier, infection of the nervous system, and simultaneous attack and replication in different parenchymal tissues and organs (Teijaro et al., 2011, Tarek et al., 2021). In our study, all H5N8 viruses could satisfactorily replicate systematically in all organs tested (trachea, brain, lung, and spleen) with high viral titer and showed more pathological changes in the trachea, lung, spleen, and brain of F446-infected chickens at 2 and 4 dpi than in chickens inoculated with other H5N8 viruses. The histopathological changes were characterized by inflammatory and necrotizing changes, which occur owing to invasion and replication of the virus in the cells of different organs.

Considering these previous findings, the following could be proposed for efficient replication, comparable pathogenicity of F446-like strains; first, early adaptation by serial passage in commercial ducks where these strains can silently spread with efficient transmission to other birds; and second, the more adapted unique polymerase complex is a result of the different origins of the NP and PA genes. Both scenarios require future studies based on direct surveillance of ducks in backyards and commercial farms. Studies examining the impact of different polymerase reassortments using reverse genetic approaches are also required.

CONCLUSION

Based on the comparative pathogenesis analysis, the replication and transmissibility of the three HPAI H5N8 viruses conclusively showed that the F446-like strains are relatively more pathogenic and efficient in replication and transmissibility than other H5N8 viruses. In addition, more pathological changes in chickens were caused by low CLD50, as well as high mortality rate and high viral titer in swabs and samples obtained from infected organs.

ACKNOWLEDGMENTS

Prof. Khaled A. El-Tarabily thanks library at Murdoch University, Australia for the valuable online resources and comprehensive databases.

DISCLOSURES

The authors declare no conflict of interest.

REFERENCES

Bouwstra, R. J., G. Koch, R. Heutink, F. Harders, A. Van Der Spek, A. R. Elbers, and A. Bossers. 2015. Phylogenetic analysis of highly pathogenic avian influenza A (H5N8) virus outbreak strains provides evidence for four separate introductions and one between-poultry farm transmission in the Netherlands, November 2014. Euro. Surveill. 20:21174.

Chan, Y. H. 2003. Biostatistics 102: quantitative data−parametric & non-parametric tests. Singapore Med. J. 44:391–396.

Chan, Y. H. 2004. Biostatistics 203. Survival analysis. Singapore Med. J. 45:249–256.

Gu, M., W. Liu, Y. Cao, D. Peng, X. Wang, H. Wan, G. Zhao, Q. Xu, W. Zhang, Q. Song, Y. Li, and X. Liu. 2011. Novel reassortant highly pathogenic avian influenza (H5N5) viruses in domestic ducks, China. Emerg. Infect. Dis. 17:1060–1063.

Hagag, N. M., A. M. Erfan, M. El-Husseiny, A. G. Shalaby, M. A. Saif, M. M. Tawakol, A. A. Nour, A. A. Selim, A. S. Arafa, M. K. Hassan, W. Hassan, H. A. Fahmy, E. Ibraheem, M. Attia, A. Abdelhakim, M. A. Shahein, and M. M. Naguib. 2019. Isolation of a novel reassortant highly pathogenic avian influenza (H5N2) virus in Egypt. Viruses 11:565.

Hanna, A., J. Banks, D. A. Marston, R. J. Ellis, S. M. Brookes, and I. H. Brown. 2015. Genetic characterization of highly pathogenic avian influenza (H5N8) virus from domestic ducks, England, November 2014. Emerg. Infect. Dis. 21:879–882.

Harder, T., S. Maurer-Stroh, A. Pohlmann, E. Starick, D. Höreth-Böntgen, K. Albrecht, G. Pannwitz, J. Teifke, V. Gunalan, R. T. Lee, C. Sauter-Louis, T. Homeier, C. Staubach, C. Wolf, G. Strebelow, D. Höper, C. Grund, F. J. Conraths, T. C. Mettenleiter, and M. Beer. 2015. Influenza A (H5N8) virus similar to strain in Korea causing highly pathogenic avian influenza in Germany. Emerg. Infect. Dis. 21:860–863.

Hassan, K. E., N. Saad, H. H. Abozeid, S. Shany, M. F. El-Kady, A. Arafa, A. El-Sawah, F. Pfaff, H. M. Hafez, M. Beer, and T. Harder. 2020. Genotyping and reassortment analysis of highly pathogenic avian influenza viruses H5N8 and H5N2 from Egypt reveals successive annual replacement of genotypes. Infect. Genet. Evol. 84:104375.

Jeong, J., H. M. Kang, E. K. Lee, B. M. Song, Y. K. Kwon, H. R. Kim, K. S. Choi, J. Y. Kim, H. J. Lee, O. K. Moon, W. Jeong, J. Choi, J. H. Baek, Y. S. Joo, Y. H. Park, H. S. Lee, and Y. J. Lee. 2014. Highly pathogenic avian influenza virus (H5N8) in domestic poultry and its relationship with migratory birds in South Korea during 2014. Vet. Microbiol. 173:249–257.

Kandeil, A., A. Kayed, Y. Moatasim, R. J. Webby, P. P. McKenzie, G. Kayali, and M. A. Ali. 2017. Genetic characterization of highly pathogenic avian influenza A H5N8 viruses isolated from wild birds in Egypt. J. Gen. Virol. 98:1573–1586.

Kandeil, A., J. T. Hicks, S. G. Young, A. N. El Taweel, A. S. Kayed, Y. Moatasim, O. Kutkat, O. Bagato, P. P. McKenzie, Z. Cai, R. Badra, M. Kutkat, J. Bahl, R. J. Webby, G. Kayali, and M. A. Ali. 2019. Active surveillance and genetic evolution of avian influenza viruses in Egypt, 2016-2018. Emerg. Microbes Infect. 8:1370–1382.

Kleyheeg, E., R. Slaterus, R. Bodewes, J. M. Rijks, M. A. Spierenburg, N. Beerens, L. Kelder, M. J. Poen, J. A. Stegeman, R. Fouchier, T. Kuiken, and H. P. van der Jeugd. 2017. Deaths among wild birds during highly pathogenic avian influenza A (H5N8) virus outbreak, the Netherlands. Emerg. Infect. Dis. 23:2050–2054.

Landmann, M., D. Scheibner, A. Graaf, M. Gischke, S. Koethe, O. I. Fatola, B. Raddatz, T. C. Mettenleiter, M. Beer, C. Grund, and T. Harder. 2021. A semiquantitative scoring system for histopathological and immunohistochemical assessment of lesions and tissue tropism in avian influenza. Viruses 13:868.

Lee, D. H., J. Bahl, M. K. Torchetti, M. L. Killian, H. S. Ip, T. J. DeLiberto, and D. E. Swayne. 2016. Highly pathogenic avian influenza viruses and generation of novel reassortants, United States, 2014−2015. Emerg. Infect. Dis. 22:1283–1285.

Lee, D. H., K. Bertran, J. H. Kwon, and D. E. Swayne. 2017a. Evolution, global spread, and pathogenicity of highly pathogenic avian influenza H5Nx clade 2.3. 4.4. J. Vet. Sci. 18:269–280.

Lee, D. H., K. Sharshov, D. E. Swayne, O. Kurskaya, I. Sobolev, M. Kabilov, A. Alekseev, V. Irza, and A. Shestopalov. 2017b.

Novel reassortant clade 2.3. 4.4 avian influenza A (H5N8) virus in wild aquatic birds, Russia, 2016. Emerg. Infect. Dis. 23:359–360.

Li, M., H. Liu, Y. Bi, J. Sun, G. Wong, D. Liu, L. Li, J. Liu, Q. Chen, H. Wang, Y. He, W. Shi, G. F. Gao, and J. Chen. 2017. Highly pathogenic avian influenza A (H5N8) virus in wild migratory birds, Qinghai Lake, China. Emerg. Infect. Dis. 23:637–641.

Löndt, B. Z., A. Nunez, J. Banks, H. Nili, L. K. Johnson, and D. J. Alexander. 2008. Pathogenesis of highly pathogenic avian influenza A/turkey/Turkey/1/2005 H5N1 in Pekin ducks (*Anas platyrhynchos*) infected experimentally. Avian Pathol. 37:619–627.

OIE (Office International des Epizooties). 2017. Update on Highly Pathogenic Avian Influenza in Animals (Type H5 and H7). Accessed Mar. 2021. http://www.oie.int/animal-health-in-the-world/update-on-avian-influenza/2017/. 2017.

OIE, World Organization for Animal Health. 2018. Avian influenza—infection with avian influenza viruses. Pages 821−84 in Manual of Diagnostic Tests and Vaccines for Terrestrial Animals 2018. Accessed Mar. 2019. https://www.oie.int/fileadmin/Home/eng/Health_standards/tahm/3.03.04_AI.pdf

Pasick, J., Y. Berhane, T. Joseph, V. Bowes, T. Hisanaga, K. Handel, and S. Alexandersen. 2015. Reassortant highly pathogenic influenza A H5N2 virus containing gene segments related to Eurasian H5N8 in British Columbia, Canada, 2014. Sci. Rep. 5:1–4.

Pohlmann, A., E. Starick, T. Harder, C. Grund, D. Höper, A. Globig, C. Staubach, K. Dietze, G. Strebelow, R. G. Ulrich, J. Schinköthe, J. P. Teifke, F. J. Conraths, T. C. Mettenleiter, and M. M. Beer. 2017. Outbreaks among wild birds and domestic poultry caused by reassorted influenza A (H5N8) clade 2.3. 4.4 viruses, Germany, 2016. Emerg. Infect. Dis. 23:633–636.

Reed, L. J., and H. Muench. 1938. A simple method of estimating fifty percent endpoints. Am. J. Epidemiol. 27:493–497.

Röhm, C., T. Horimoto, Y. Kawaoka, J. Süss, and R. G. Webster. 1995. Do hemagglutinin genes of highly pathogenic avian influenza viruses constitute unique phylogenetic lineages? Virology 209:664–670.

Salaheldin, A. H., H. S. Abd El-Hamid, A. R. Elbestawy, J. Veits, H. M. Hafez, T. C. Mettenleiter, and E. M. Abdelwhab. 2018. Multiple introductions of influenza A (H5N8) virus into poultry, Egypt, 2017. Emerg. Infect. Dis. 24:943–946.

Selim, A. A., A. M. Erfan, N. Hagag, A. Zanaty, A. H. Samir, M. Samy, A. Abdelhalim, A. A. Arafa, M. A. Soliman, M. Shaheen, E. M. Ibraheem, I. Mahrous, M. K. Hassan, and M. M. Naguib. 2017. Highly pathogenic avian influenza virus (H5N8) clade 2.3. 4.4 infection in migratory birds, Egypt. Emerg. Infect. Dis. 23:1048–1051.

Silvano, F. D., M. Yoshikawa, A. Shimada, K. Otsuki, and T. Umemura. 1997. Enhanced neuropathogenicity of avian influenza A virus by passages through air sac and brain of chicks. J. Vet. Med. Sci. 59:143–148.

Song, B. M., H. M. Kang, E. K. Lee, J. Jeong, Y. Kang, H. S. Lee, and Y. J. Lee. 2015. Pathogenicity of H5N8 virus in chickens from Korea in 2014. J. Vet. Sci. 16:237–240.

Swayne, D. E., G. R. Gillson, M. W. Jackwood, and J. E. Pearson. 1998. A Laboratory Manual for the Isolation and Identification of Avian Pathogens. 4th ed. American Association of Avian Pathologists, PA, USA, 400 pp.

Swayne, D. E., M. J. Radin, T. M. Hoepf, and R. D. Slemons. 1994. Acute renal failure as the cause of death in chickens following intravenous inoculation with avian influenza virus A/chicken/Alabama/7395/75 (H4N8). Avian Dis. 38:151–157.

Swayne, D., K. Bertran, D. Kapczynski, M. Pantin-Jackwood, E. Spackman, D. H. Lee, and D. Suarez. 2016. Impact of emergence of avian influenza in North America and preventative measures. Pages 24-27 in Proceedings of the Sixty-Fifth Western Poultry Disease Conference. D. E. Swayne, ed.Vancouver, BC, Canada.

Tanikawa, T., K. Kanehira, R. Tsunekuni, Y. Uchida, N. Takemae, and T. Saito. 2016. Pathogenicity of H5N8 highly pathogenic avian influenza viruses isolated from a wild bird fecal specimen and a chicken in Japan in 2014. Microbiol. Immunol. 60:243–252.

Tarek, M., M. M. Naguib, A. Arafa, L. A. Tantawy, K. M. Selim, S. Talaat, and H. A. Sultan. 2021. Epidemiology, genetic characterization, and pathogenesis of avian influenza H5N8 viruses circulating in northern and southern parts of Egypt, 2017−2019. Animals 11:2208.

Teijaro, J. R., K. B. Walsh, S. Cahalan, D. M. Fremgen, E. Roberts, F. Scott, E. Martinborough, R. Peach, M. B. Oldstone, and H. Rosen. 2011. Endothelial cells are central orchestrators of cytokine amplification during influenza virus infection. Cell 146:980–991.

Vigeveno, R. M., M. J. Poen, E. Parker, M. Holwerda, K. de Haan, T. van Montfort, N. S. Lewis, C. A. Russell, R. A. M. Fouchier, M. D. de Jong, and D. Eggink. 2020. Outbreak severity of highly pathogenic avian influenza A(H5N8) viruses is inversely correlated to polymerase complex activity and interferon induction. J. Virol. 94 e00375-20.

WHO (World Health Organization). 2008. H5N1 Avian Influenza: Timeline of Major Events, accessed date 16 Dec 2008. https://www.who.int/influenza/human_animal_interface/avian_influenza/H5N1_avian_influenza_update.pdf

WHO. 2020. Human Infection With Avian Influenza A(H5) Viruses, Accessed Apr. 2020. https://www.who.int/docs/default-source/wpro—documents/emergency/surveillance/avian-influenza/ai-20200424.pdf?sfvrsn=223ca73f_48.

Wu, H., X. Peng, L. Xu, C. Jin, L. Cheng, X. Lu, T. Xie, H. Yao, and N. Wu. 2014. Novel reassortant influenza A (H5N8) viruses in domestic ducks, eastern China. Emerg. Infect. Dis. 20:1315–1318.

Yehia, N., M. M. Naguib, R. Li, N. Hagag, M. El-Husseiny, Z. Mosaad, A. Nour, N. Rabea, W. M. Hasan, M. K. Hassan, T. Harder, and A. A. Arafa. 2018. Multiple introductions of reassorted highly pathogenic avian influenza viruses (H5N8) clade 2.3. 4.4 b causing outbreaks in wild birds and poultry in Egypt. Infect. Genet. Evol. 58:56–65.

Yehia, N., W. M. M. Hassan, A. Sedeek, and M. H. Elhusseiny. 2020. Genetic variability of avian influenza virus subtype H5N8 in Egypt in 2017 and 2018. Arch. Virol. 165:1357–1366.

Zhao, G., X. Gu, X. Lu, J. Pan, Z. Duan, K. Zhao, M. Gu, Q. Liu, L. He, J. Chen, S. Ge, Y. Wang, S. Chen, X. Wang, D. Peng, H. Wan, and X. Liu. 2012. Novel reassortant highly pathogenic H5N2 avian influenza viruses in poultry in China. PLoS One 7: e46183.